REPORT DOCUMENTATION PAGE

Form Approved OMB NO. 0704-0188

1. REPORT DATE (DD-MM-YYYY)	2. REPORT TYPE	3. DATES COVERED (From - To)
17-08-2013	Final Report	1-Sep-2012 - 31-May-2013

4. TITLE AND SUBTITLE
Synchronization of Two Remote Nanomechanical Oscillators

5a. CONTRACT NUMBER
W911NF-12-1-0490

5b. GRANT NUMBER

5c. PROGRAM ELEMENT NUMBER
611102

6. AUTHORS
Hong Tang

5d. PROJECT NUMBER

5e. TASK NUMBER

5f. WORK UNIT NUMBER

7. PERFORMING ORGANIZATION NAMES AND ADDRESSES
Yale University
Office of Grant & Contract Administration
47 College Street, Suite 203
New Haven, CT 06520 -8047

8. PERFORMING ORGANIZATION REPORT NUMBER

9. SPONSORING/MONITORING AGENCY NAME(S) AND ADDRESS(ES)
U.S. Army Research Office
P.O. Box 12211
Research Triangle Park, NC 27709-2211

10. SPONSOR/MONITOR'S ACRONYM(S)
ARO

11. SPONSOR/MONITOR'S REPORT NUMBER(S)
62584-EG-II.2

12. DISTRIBUTION AVAILIBILITY STATEMENT
Approved for Public Release; Distribution Unlimited

13. SUPPLEMENTARY NOTES
The views, opinions and/or findings contained in this report are those of the author(s) and should not contrued as an official Department of the Army position, policy or decision, unless so designated by other documentation.

14. ABSTRACT
The goal of this pilot project is to demonstrate unambiguous synchronization between two nanoscale mechanical oscillators. In the system we studied, two mechanical resonators are remotely placed and linked in a closed-loop photonic bus waveguide, which can be treated as a photonic cavity. A programmable optical field is used to achieve controlled coupling between the two resonators via delayed optical force. The optical backaction force induces both displacement coupling and velocity coupling, and gives rise to much richer dynamics than previous studied system

15. SUBJECT TERMS
synchronization, oscillators, coupled resonators

16. SECURITY CLASSIFICATION OF:			17. LIMITATION OF ABSTRACT	15. NUMBER OF PAGES	19a. NAME OF RESPONSIBLE PERSON
a. REPORT	b. ABSTRACT	c. THIS PAGE			Hongxing Tang
UU	UU	UU	UU		19b. TELEPHONE NUMBER 203-432-4256

Report Title

Synchronization of Two Remote Nanomechanical Oscillators

ABSTRACT

The goal of this pilot project is to demonstrate unambiguous synchronization between two nanoscale mechanical oscillators. In the system we studied, two mechanical resonators are remotely placed and linked in a closed-loop photonic bus waveguide, which can be treated as a photonic cavity. A programmable optical field is used to achieve controlled coupling between the two resonators via delayed optical force. The optical backaction force induces both displacement coupling and velocity coupling, and gives rise to much richer dynamics than previous studied system where the coupling occurs in only one degree of freedom.

Enter List of papers submitted or published that acknowledge ARO support from the start of the project to the date of this printing. List the papers, including journal references, in the following categories:

(a) Papers published in peer-reviewed journals (N/A for none)

Received	Paper

TOTAL:

Number of Papers published in peer-reviewed journals:

(b) Papers published in non-peer-reviewed journals (N/A for none)

Received	Paper

TOTAL:

Number of Papers published in non peer-reviewed journals:

(c) Presentations

Number of Presentations: 0.00

Non Peer-Reviewed Conference Proceeding publications (other than abstracts):

Received	Paper

TOTAL:

Number of Non Peer-Reviewed Conference Proceeding publications (other than abstracts):

Peer-Reviewed Conference Proceeding publications (other than abstracts):

Received	Paper

TOTAL:

Number of Peer-Reviewed Conference Proceeding publications (other than abstracts):

(d) Manuscripts

Received	Paper	
08/17/2013	1.00	Mahmood Bagheri, , Menno Poot, Linran Fan, Florian Marquardt, Hong X. Tang. Photonic Cavity Synchronization of Nanomechanical Oscillators, Physical Review Letters (submitted) (08 2013)

TOTAL: **1**

Number of Manuscripts:

Books

Received	Paper

TOTAL:

Patents Submitted

Patents Awarded

Awards

Elected Member, Connecticut Academic of Science and Engineering (CASE), 2013

Graduate Students

NAME	PERCENT_SUPPORTED	Discipline
Linran Fan	0.25	
FTE Equivalent:	**0.25**	
Total Number:	**1**	

Names of Post Doctorates

NAME	PERCENT_SUPPORTED
Menno Poot	0.10
FTE Equivalent:	**0.10**
Total Number:	**1**

Names of Faculty Supported

NAME	PERCENT_SUPPORTED	National Academy Member
Hong Tang	0.00	
FTE Equivalent:	**0.00**	
Total Number:	**1**	

Names of Under Graduate students supported

NAME	PERCENT_SUPPORTED
FTE Equivalent:	
Total Number:	

Student Metrics

This section only applies to graduating undergraduates supported by this agreement in this reporting period

The number of undergraduates funded by this agreement who graduated during this period:	0.00
The number of undergraduates funded by this agreement who graduated during this period with a degree in science, mathematics, engineering, or technology fields:.....	0.00
The number of undergraduates funded by your agreement who graduated during this period and will continue to pursue a graduate or Ph.D. degree in science, mathematics, engineering, or technology fields:.....	0.00
Number of graduating undergraduates who achieved a 3.5 GPA to 4.0 (4.0 max scale):	0.00
Number of graduating undergraduates funded by a DoD funded Center of Excellence grant for Education, Research and Engineering:	0.00
The number of undergraduates funded by your agreement who graduated during this period and intend to work for the Department of Defense	0.00
The number of undergraduates funded by your agreement who graduated during this period and will receive scholarships or fellowships for further studies in science, mathematics, engineering or technology fields:	0.00

Names of Personnel receiving masters degrees

NAME

Total Number:

Names of personnel receiving PHDs

NAME

Total Number:

Names of other research staff

NAME PERCENT_SUPPORTED

FTE Equivalent:

Total Number:

Sub Contractors (DD882)

Inventions (DD882)

Scientific Progress

See attachment

Technology Transfer

Project report for Award ARO-STIR W911NF1210490

Project title: Synchronization of Two Remote Nanomechanical Oscillators

Principle investigator: Dr. Hong Tang, Associate Professor,
Department of Electrical Engineering
Tel: 203-432-4256, Fax: 203-432-7769, email: hong.tang@yale.edu
Yale University, 15 Prospect St, New Haven, CT 06520

Other personnel involved: Mahmood Bagheri, Menno Poot, Linran Fan, Florian Marquardt

Duration of effort: Oct 1 2012-June 30 2013 for 9 months

The goal of this pilot project is to demonstrate unambiguous synchronization between two nanoscale mechanical oscillators. In the system we studied, two mechanical resonators are remotely placed and linked in a closed-loop photonic bus waveguide, which can be treated as a photonic cavity. A programmable optical field is used to achieve controlled coupling between the two resonators via delayed optical force. The optical backaction force induces both displacement coupling and velocity coupling, and gives rise to much richer dynamics than previous studied system where the coupling occurs in only one degree of freedom.

1. Introduction of the proposed scope of research

Synchronization is a ubiquitous phenomenon where the phase difference between free-running oscillators remains constant due to the mutual coupling. Besides its well-accepted importance in biological sciences, today synchronization is becoming a powerful tool for many engineered systems[1]. For instance, synchronization is desirable in situations where high oscillating power, strong coherence, or low phase noise are needed, such as lasers[2], phase-locked loops[3], Josephson junction arrays[4], and spin-torque resonators[5]. Synchronization also promises to improve the accuracy of time-keeping devices[6]. Since the observations of synchronization in pendulums[7] this concept has found its bearings in science and engineering due to its potential applications in generating low-noise stable oscillating signals. Nanomechanical oscillators, on the other hand, are very appealing as they simultaneously offer high quality factor resonances, excellent scalability[8,9] and are ideal systems for synchronization studies due to their highly engineerable nonlinearities[10].

However, achieving reproducible and strong coupling in nanomechanical devices remains

difficult due to the unavoidable device non-uniformity and weak mutual coupling. This can be circumvented by coupling nanomechanical resonators to an optical cavity[11]. Recently, synchronization between two closely spaced micromechanical resonators was demonstrated using a hybrid optical mode of two coupled disk resonators and the synchronization phase-space was predicted using the Kuramoto model[12]. Here we experimentally demonstrate the first synchronization of two spatially separated nanoscale radio-frequency oscillators integrated inside an optical racetrack cavity. We show that this leads to a limit cycle in the reduced three-dimensional mechanical phase space (The two mechanical resonators' amplitudes and their phase difference[13]) and that the dynamics of two mechanical modes coupled via a common optical mode cannot be captured by the standard Kuramoto model[14]: as a result of the additional degrees of freedom of the coupled system, slow dynamics appear on top of the limit cycle, and sidebands emerge. These sidebands are true signatures of synchronized motion in the mechanical domain and are not to be confused with simple nonlinear intermodulation oscillatory modes. Their presence is important for the phase noise performance of synchronized optomechanical oscillators, and could counteract the common perception that synchronized states should always improve phase noise performance.

2. Our experimental research and main findings

We investigate the interaction between two MHz-frequency nanomechanical resonators that are linked in an optical racetrack (Fig. 1(a)); The resonators are mechanically isolated, due to their large separation (~ 80 μm), ensuring that any coupling between them is through the optical field. The fabrication of these integrated photonic devices is readily scalable [1, [15]], making this an ideal platform for synchronization studies [11, 14]. The silicon beams are slightly buckled and they may end up in the up or down state (Fig. 1(a)).

The measurement setup shown in Fig. 1d consists of a strong pump laser to create cavity backaction and a weak probe to detect the motion [13]. First the two nanomechanical resonators are characterized with the pump laser off, so that the backaction is small. When the two resonators are both in the buckled-up state their resonance frequencies are close with a small difference due to fabrication imperfections (6.53 MHz vs. 6.61 MHz) as indicated by the thermal displacement noise spectrum in Fig. 1(b). However, when one resonator is displaced from the up state to the down state, its mechanical resonance frequency drops to 4.05 MHz (Fig. 1(c)) due to

asymmetries of the double-well potentials. The intrinsic damping rate of the resonators $\gamma/2\pi \sim 2$ kHz [13].

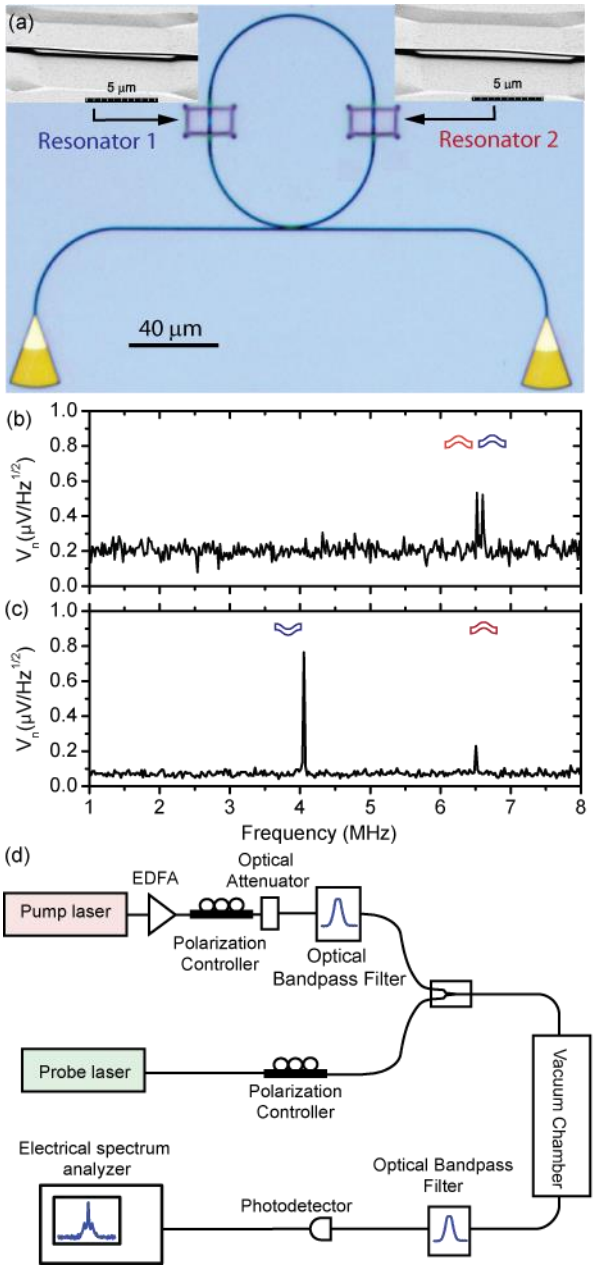

Figure 1. (a) Micrograph of a racetrack cavity with two 110nm x 500nm x 10um suspended portions as nanomechanical resonators. Insets show scanning electron micrographs of the mechanical resonators in buckled down (left) and buckled up (right) state. (b,c) thermal noise spectra in the up-up (b**)** down-up state (c). (d) The measurement setup with a weak probe laser, and a pump.

Optomechanical oscillators (OMOs) in single cavity, single resonator systems have been the subject of intense studies in recent years [[16], [17], [18]]. It is, however, expected that when multiple oscillators are embedded in a single cavity new phenomena will appear due to the mutual

coupling via the cavity field. Figure 2a displays the evolution of the RF power spectrum of the transmitted probe laser light (the pump laser is blue detuned at $\Delta_0/\kappa = 0.3$, where Δ_0 is the detuning between the laser and cavity frequency, and κ is the cavity linewidth). At the lowest pump powers the thermomechanical motion of each resonator is visible as two lines at 4.0 and 6.5 MHz respectively. Upon increasing the pump power in this first regime, their Brownian motion is amplified as the backaction reduces the damping. Also, the optical spring effect [19] is visible as an increase in the resonance frequencies. Both effects are stronger in the 4 MHz resonator since in the buckled down state the effective refractive index of the racetrack depends more strongly on the displacement yielding a larger optomechanical coupling g_{om}; From simulations we estimate $g_{\mathrm{om}}/2\pi$ = 140 and 500 MHz/nm for up and down. The difference in backaction confirms that optical backaction is stronger than photothermal effects as the latter would be the same on both resonators, irrespective of their separation from substrate[20].

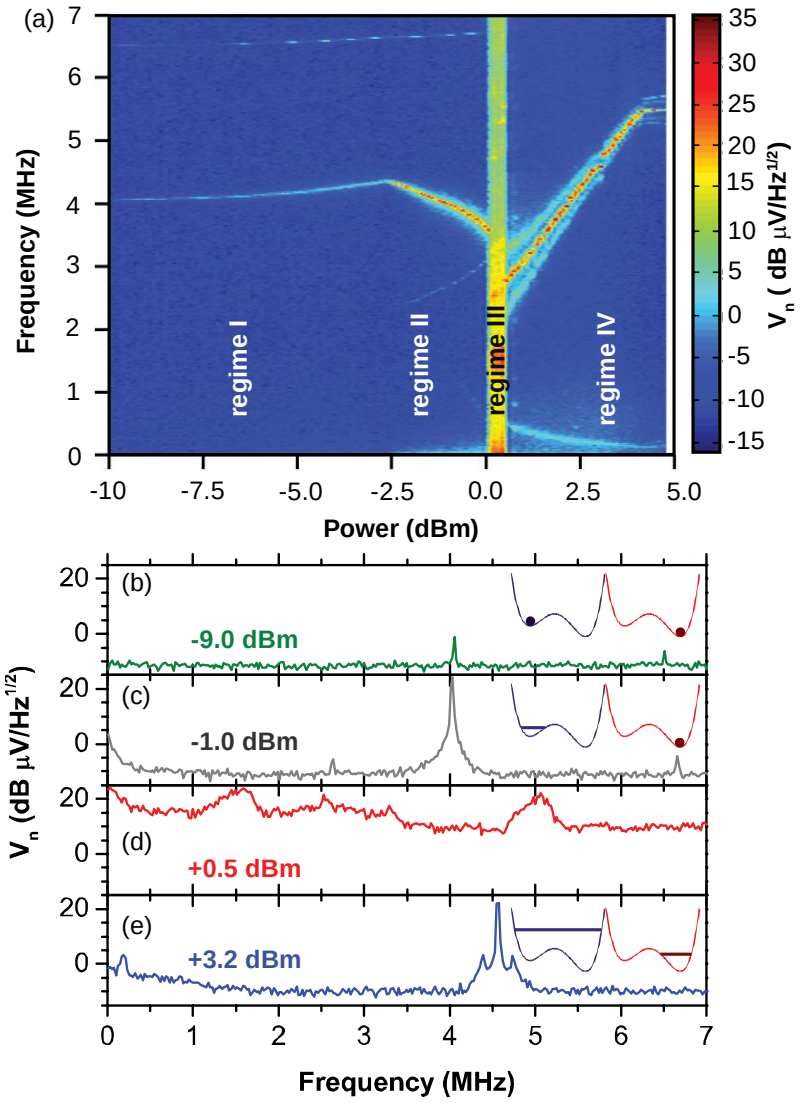

Figure 2. (a) The evolution of the RF power spectrum of the transmitted light as the pump power increases. (b)-(e) Cuts through panel (a) at the indicated pump power when both resonators are in a thermal state (regime I, (b)), (c) one resonator is in thermal motion while the other resonator experiences regenerative oscillations (regime II), (d) the chaotic regime (III) and (e) the two resonators are synchronized (regime IV). The insets schematically show the energy of resonators 1 (left) and 2 (right); dots correspond to small thermal motion, and lines to large oscillations.

When the pump is increased beyond -2.7dBm, the optomechanical gain fully compensates the mechanical damping of the resonator with the lowest threshold, which we will label as "1", which starts to self-oscillate. This demarcates the onset of regime II which ranges from -2.7 dBm to 0.2 dBm. Yet, even though the oscillation amplitude of resonator 1 increased dramatically, the

thermal motion of resonator 2 is undisturbed and is still clearly visible in Fig. 2(a) and (b). Note, that the frequency difference between the two resonators (2.5 MHz) is much larger than the spectral width of resonator 2, so the cavity occupation oscillation induced by OMO 1 cannot efficiently drive the other resonator. Regime II thus corresponds to the single oscillator system that we studied previously. One might expect that resonator 2 simply starts to oscillate when the power is increased beyond the second threshold which is higher due to its lower g_{om}. Instead, different dynamics is encountered (Regime III) where the power spectrum displays a large magnitude over a wide range of frequencies. Here, the motion is chaotic and the phase, amplitude, and frequency of the transmitted probe light change on short timescales. This chaotic behavior only exists for a limited power range and vanishes beyond 0.7 dBm.

Above 0.7dBm the two oscillators start their synchronized motion, as evidenced by a dramatic change in the mechanical displacement spectrum. In Regime IV the detected photocurrent contains a strong narrow tone and, more importantly, the thermomechanical motion of resonator 2 is now no longer visible. The single strong peak in the RF spectrum indicates that both resonators are oscillating at the same frequency; In this case they are said to be synchronized since the phase difference between them remains constant. We have thus synchronized the two resonators despite the extremely large frequency difference: the second mode, originally at 6.7 MHZ, was almost twice as fast as the oscillations of the first mode at 3.9 MHz, indicating the extremely strong optomechanical interactions and the tunability of the double well potential in our system. Note, that in previous micromechanical synchronization experiments the frequency difference was limited to ~0.2% [12].

The spectra in Regime IV also reveal another surprise: Sidebands emerge around the strongest peak (the carrier), indicating a modulation of the self-sustained oscillations. A close inspection of Fig. 2(a) and (e) shows that the spectra contain two equally spaced sidebands ~100-500 kHz from the carrier. Their presence implies a deteriorated signal phase noise at that particular sideband offset frequency [21]. These weak (~20-35 dBc), but clearly defined, sidebands are not transient phenomena as they persist during the entire data-acquisition time, which is much longer than the damping time of the resonator γ^{-1}. Also, in Regime II (Fig. 2(c)) with only a single OMO present, sidebands are absent, ruling out low-frequency thermal instabilities [22] interfering with optomechanical oscillations. Finally, the mixing of the sidebands in Regime IV with the

strong carrier produces a signal below 500 kHz). This down-converted peak is not mechanical in origin but is due to the nonlinearity of the transduction at large amplitudes. Similarly, in Regime II the thermal motion of resonator 2 is mixed with that of OMO 1, resulting in a peak near 2.5 MHz.

3. Theoretical analysis of photonic cavity coupled nanomechanical oscillators

To understand the origin of synchronization and the slow dynamics in the cavity-coupled oscillators we theoretically analyse this system; for details see [13]. Multiple uncoupled oscillators will each oscillate at their own frequency, but the cavity field couples the oscillators enabling synchronization as will be shown. When the frequency difference between the resonators $\upsilon \ll \bar{\Omega}$, the equation of motion for their complex amplitude $U_k = g_{om,k}\langle(u_k + \dot{u}_k/i\bar{\Omega})\exp(-\mathrm{i}\bar{\Omega}\mathrm{t})\rangle = A_k \exp(i\theta_k)$ in the frame rotating at the average frequency $\bar{\Omega} = \frac{1}{2}(\Omega_1 + \Omega_2)$ is [14, [23],[24]]:

$$\dot{U}_{1,2} = \pm i\frac{\upsilon}{2}U_{1,2} - \frac{\gamma_{1,2}}{2}U_{1,2} - i\bar{\Omega}c_{om,1,2}\Phi(\mathrm{t}), \qquad (1)$$

where u_k are the displacements of the two resonators (k=1,2). and $\Phi(\mathrm{t})$ describes how the photon occupation responds to a dynamic displacement [24]. $c_{om,k} = \hbar n_{\max} g_{om,k}^2/m_k\bar{\Omega}^3$ are the coupling strengths *and* $n_{\max}$ is the maximum number of photons in the cavity. When multiple resonators are present, the cavity only feels the *combined* effect of all resonators. The same reasoning as for a single OMO shows that for multiple resonators coupled to the same cavity, the cavity response is $\Phi(\mathrm{t}) = \Phi(A_+(t))$ where A_+ is the magnitude of the summed complex amplitude $U_+(t) = \sum_k U_k(t) = A_+(t)\exp(\mathrm{i}\theta_+(t))$. A_+ depends on the phase difference between the individual oscillators, but not on the overall phase θ_+. The equations of motion for the two OMOs are thus coupled together via U_+ and the cavity response function $\Phi(\mathrm{A}_+)$. Synchronized motion of the two oscillators implies that they rotate at the same frequency $\bar{\Omega} + \epsilon$. Hence, $U_{1,2}(t) = Y_{1,2}\exp(i\epsilon t)$ must be a solution to Eq. (1): if no such solution exists, synchronization cannot take place. Inserting the solution into Eq. (1) yields the equation that determines the combined amplitudes of the limit cycles:

$$\Phi(\mathrm{A}_+) = \frac{1}{\bar{\Omega}} \frac{\left(\frac{\upsilon}{2}\right)^2 - \epsilon^2 + i\epsilon\bar{\gamma} + \frac{i\,\delta\,\gamma\nu}{4} + \left(\frac{\bar{\gamma}}{2}\right)^2 - \left(\frac{\delta\gamma}{4}\right)^2}{2\epsilon\bar{c}_{om} + \nu\frac{\delta c_{om}}{2} + i\frac{\delta c_{om}}{2}\frac{\delta\,\gamma}{2} - i\bar{\gamma}\bar{c}_{om}}, \qquad (2)$$

where $\bar{c}_{om}$ (δc_{om}) and $\bar{\gamma}$ ($\delta\gamma$) are the average (difference in) coupling strengths and damping rates respectively. Solving Eq. (2) can be done as illustrated in Fig. 3(a); the left hand side is a curve in the complex plane parameterized by A_+ (for a given detuning and decay rate), whereas the right hand side depends only on the oscillators' properties and is parameterized by the unknown frequency ϵ. Intersections of the two curves are thus solutions to Eq. (2). When inserting the obtained values for A_+ and ϵ back into Eq. (1) the individual contributions Y_1 and Y_2 can be obtained including their phases relative to the carrier $Y_+ = Y_1+Y_2$. Fig. 3(b) shows that for the parameters of Fig. 3(a) the two complex amplitudes Y_1 and Y_2 have a similar, but not identical, magnitude and oscillator 1 moves ahead of the second. Finally, for sufficiently asymmetric oscillators, the two curves can intersect more than once, leading to multistability [22,23], even in the unresolved sideband regime where a single oscillator always has a unique amplitude.

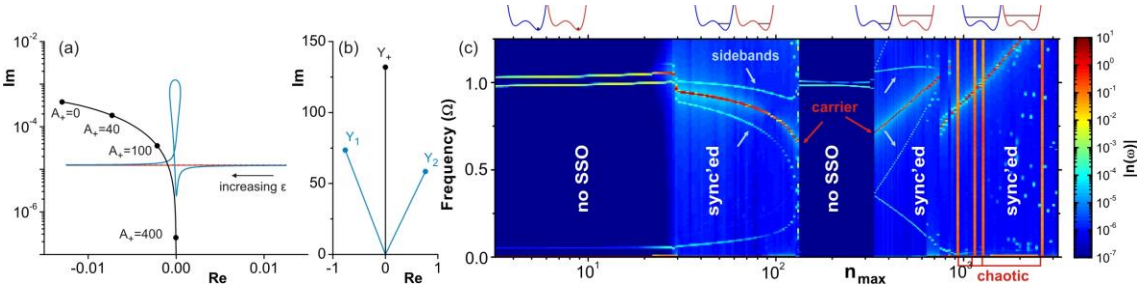

Figure 3. (a) Complex plane representation of the cavity response $\Phi(\mathrm{A}_+)$ (black) and the right hand side of Eq. (5) for two identical oscillators (red) and two oscillators with $\bar{\gamma}$ = 0.001 $\bar{\Omega}$, $\bar{c}_{om}$ = 20, υ = 0.01 $\bar{\Omega}$, $\delta\,\gamma$ = 0.0018 $\bar{\Omega}$, and δc_{om} = 0 (blue). The curves intersect at A_+ = 132.0 and ϵ = 0.0438 $\bar{\Omega}$ (b) Complex amplitudes of the individual oscillators for the solution shown in (a). (c) Colorplot of the Fourier transform of the photon number on a logarithmic scale. The carrier tone and its sidebands are indicated by red and white arrows respectively. The parameters are: $Q_1 = Q_2$ = 6000, κ = 526 $\bar{\Omega}$, Δ_0 = 0.493κ, $g_{\mathrm{om},1} = g_{\mathrm{om},2}$ = 1.

Equation (2) thus yields the fixed points with synchronization. However, to understand the dynamics around the corresponding limit cycle, Eq. (1) can be expanded for small excursions and the eigenvalues can be found. There are three independent degrees of freedom: the two oscillation amplitudes and the phase difference between them. The fourth degree of freedom, the overall phase θ_+, is not fixed yielding a zero eigenvalue. Depending on the values of the other

three eigenvalues different types of behavior are possible: returning back to the fixed point without oscillations (overdamped), returning with oscillations (underdamped), or the fixed point is unstable. In the second case, when any of the two oscillators is displaced, e.g. due to the ever-present stochastic thermal force or photon shot noise, it will return back to the fixed point in an oscillatory fashion, which shows up as sidebands in the frequency domain. In contrast, for a single oscillator, there is only one mechanical degree of freedom, the oscillation amplitude A and the corresponding eigenvalue is always real. Any small deviation thus overdampedly returns to the limit cycle and no sidebands are generated [23].

The analytical model thus hints that the observed sidebands are due to the thermal force noise acting on the oscillators. To further analyze the synchronization dynamics, the full coupled equation of motion of the mechanical resonators and that of the cavity field (cf. Eqs. (S1) and (S2)) are integrated numerically (see Supplemental Material [13]) with mechanical nonlinearities included. We chose to simulate a conceptually clear situation with nearly identical resonators (5% frequency difference and identical g_{om}). The effect of (thermal) force noise is accounted for by kicking the resonators away from their steady state oscillations. Figure 3(c) shows the evolution of the light field power spectrum as a function of n_{max} (i.e., the pump power). Similar to the experiment (Fig. 2), at low power two weak peaks are visible which also tune upwards with increasing power due to the optical spring effect. Around n_{max} = 30 oscillations start, but now the two resonators immediately oscillate simultaneously [25]. As expected from our analytical theory of synchronized motion, sidebands appear in the spectrum, but only when kicks are included. As illustrated in [13] the oscillators are truly phase locked in this regime, indicating full synchronization. When further increasing n_{max} the oscillations grow towards the top of the potential barriers and hence the frequency goes down. When the barrier is crossed at n_{max} = 134 the detuning suddenly changes dramatically and the oscillations stop. However, they reappear at higher powers and above the barrier, just as in the experiment, the oscillation frequency increases with increasing power (see also Fig. 2a). Also note that the sidebands start out far from the carrier at the onset (n_{max} = 335) of the oscillations in this regime and that, just as in Fig. 2a, they converge towards the carrier with increasing power. Finally, the simulations also reproduce bands with chaotic behavior with broad spectrums similar to the one in Fig. 2(d). The simulations thus qualitatively reproduce most of the features observed in the experiment, including the correct tuning behavior of the resonance frequency, the appearance of the

sidebands of the synchronized resonators due to thermal force noise, and chaos. It is expected that even better agreement could be reached if the exact shapes of the mechanical potentials were known, and by including displacement-dependent optomechanical coupling coefficients, although we have to leave this to future work.

We have also studied the dynamics of a single mechanical oscillator in the presence of an external oscillator encoded in the light field. This is extremely important in the context of synchronizing a remote oscillator to an external clock and also further validates our model for optomechanical synchronization. To this end, the pump power is set between the oscillation thresholds of the first and second resonator (so that the latter does not play a role) and is modulated at frequency Ω_0 = 6.800 MHz. When the modulation index (m) is zero, resonator 1 oscillates freely in the up-state at 6.804 MHz as shown in the bottom spectrum in Fig. 4. However, when the modulation is switched on the oscillations jump to Ω_0, synchronizing the OMO to the external clock. Interestingly, sidebands appear again. A prominent feature that the location of the sidebands is not constant: the offset frequency increases with m. All of this is reproduced in the numerical simulations [13] showing that many of the phenomena observed in the two-OMO case can also understood in the conceptually simpler injection locking experiments [[26]].

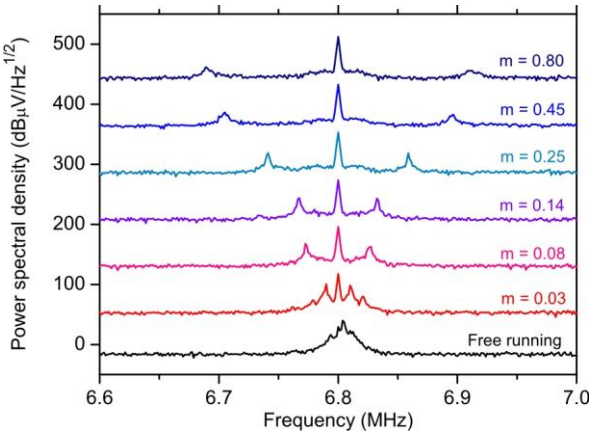

Figure 4. Measured RF power spectral density of the detector output with a free running oscillator (black) and oscillations in the presence of an increasingly larger modulation depth of the pump (red to dark blue) for constant *average* power. The curves are offset for clarity.

4. Prospect and future plans

Our technique of coupling mechanical oscillators via a single photonic bus creates a whole new platform for nonlinear studies. It will enable synchronization of large arrays of individual optomechanical elements with interesting new collective phenomena [27] and allows synchronization over arbitrarily long distances. Finally, by exploiting the memory storage capabilities of the double well resonators we envision combining the information of the mechanical bits with synchronization. This could, for example, be used to perform conditional coupling of oscillators, an interesting future direction enabled by our cavity field coupling.

11. List of References

[1] J. Kurths, A. Pikovsky, M. Rosenblum, M. *Synchronization: A Universal Concept in Nonlinear Sciences.* (Cambridge University Press, 2001).

[2] K.S. Thornburg, *et al. Phys. Rev. E* **55**, 3865 (1997).

[3] J. J. Lynch and R. A. York, *IEEE Microwave Guid. Wave Lett.* **5**, 213 (1995).

[4] A. B. Cawthorne *et al. Phys. Rev. B* **60**, 7575 (1999); H. S. J. van der Zant and R. Fazio, *Phys. Rep*. 355, 235–334 (2001).

[5] A. Slavin, *Nat. Nanotech*. **4**, 479 (2009).

[6] S. H. Strogatz, *Physica D* **143**, 1-20 (2000).

[7] Huygens, C. (Hugenii), *Horologium Oscillatorium* (Parisiis, France: Apud F. Muguet, 1967) [English translation: 1986, The Pendulum Clock (Ames: Iowa State University Press)].

[8] J. L. Arlett, E. B. Myers and M. L. Roukes, *Nat. Nanotech.* **6**, 203 (2011).

[9] X. L. Feng, C. J. White, A. Hajimiri and M. L. Roukes, *Nature Nanotech.* **3**, 342–346 (2008).

[10] R. Lifshitz, E. Kenig and M. C. Cross in *Fluctuating Nonlinear Oscillators: From Nanomechanics to Quantum Superconducting Circuits*, edited by M. I. Dykman, (Oxford University Press, Oxford, 2012), Chap 11; M. C. Cross, A. Zumdieck, R. Lifshitz and J. L. Rogers, *Phys. Rev. Lett.* **93**, 224101 (2004).

[11] C. Holmes, C. P. Meaney and G. J. Milburn, *Phys. Rev. E* **85**, 066203 (2012).

[12] M. Zhang, M. *et al. Phys. Rev. Lett.* **109**, 233906 (2012).

[13] See Supplemental Material at

[14] G. Heinrich *et al.*, *Phys. Rev. Lett.*, **107**, 043603 (2011).

[15] M. Bagheri *et al.*, *Nat. Nanotech.* **6**, 726 (2011).

[16] K. J. Vahala, *Phys. Rev. A* **78**, 023832 (2008).

[17] M. Hossein-Zadeh and K. J. Vahala, *IEEE J. of Selected Topics in Quantum Electronics* **16**, 276 (2010).

[18] Q. Lin et al., *Phys. Rev. Lett.* **103**, 103601 (2009); S. Tallur, S. Sridaran, and A. Bhave, *Optics Express*, **19**, 24522-24529 (2011).

[19] T. J. Kippenberg, and K. J. Vahala, *Science*, **321**, 1172-1176 (2008); M. Poot, and H. S. J. van der Zant, *Phys. Rep.*, **511**, 273-335 (2011).

[20] C. H. Metzger, and K. Karrai, *Nature* **432**, 1002-1005 (2004).

[21] A. Hajimiri and T. Lee, *The Design of low noise oscillators*. (Kluwer Academic Publishers, 1999).

[22] T. J. Johnson, M. Borselli, and O. Painter, *Optics Express*, **14**, 817-831 (2006).

[23] F. Marquardt, J. G. Harris and S. M. Girvin, *Phys. Rev. Lett.* **96**, 103901 (2006).

[24] M. Poot *et al.*, *Phys. Rev. A* **86**, 053826 (2012) .

[25] In the experiments the optomechanical coupling is displacement dependent and due to the asymmetry in the double-well potential there is a much larger frequency difference.

[26] M. Hossein-zadeh, and K. J. Vahala, *Appl. Phys. Lett*., **93**, 191115 (2008); M. Zalalutdinov *et al*., *Appl. Phys. Lett*. **83**, 3281 (2003).

[27] M. Ludwig and F. Marquardt, *arxiv:1208.0327*.